

## Spatial distribution of driftwood on Svalbard

Jacek URBAŃSKI ORCID-0000-0003-3842-4143

*Institute of Oceanology, Polish Academy of Sciences, Powstańców Warszawy 55, Sopot 81-712,  
Poland*

**corresponding author:** jackurbanski@iopan.com

**Received** 10 September 2025    **Accepted** 19 February 2026

**Running title:** Driftwood distribution on Svalbard

**Abstract:** The driftwood trajectories derived from a model describing sea ice drift and surface water currents show that 24% of wood logs entering the Arctic Ocean from the rivers of Western Siberia, such as the Pechora, Ob, and Yenisey, are deposited along the coasts of Svalbard. Satellite-based mapping of driftwood along the entire Svalbard coastline revealed its clustered distribution. The highest concentrations occur on the northern shores of Spitsbergen and Nordaustlandet (32%), as well as along the shores of Prins Karls Forland (24%). The majority of tree trunks, measuring 2–6 m in length, is located 20–200 m inland and at elevations of 3–8 m a.s.l. River mouths and lagoons play an important role in the local distribution of driftwood. A rough estimate suggests that Svalbard contains between 100 000 and 300 000 driftwood logs.

**Keywords:** Arctic, Svalbard archipelago, satellite-based mapping, driftwood deposition patterns, Driftwood Transport Model.

### Introduction

Driftwood (DW), defined here as tree trunks deposited along Arctic shorelines, enters the Arctic Ocean via river systems as a result of both natural processes, such as shoreline erosion and storm events, as well as logging activities (Hellmann *et al.* 2017; Stadie *et al.* 2025). Once transported into the marine environment, tree trunks may become incorporated into sea ice and

subsequently follow the trajectory of ice drift or, after release from the ice, be carried by surface currents.

The principal source of driftwood in the Spitsbergen region is the boreal forests of Siberia. Driftwood originating in that area is directly advected by the Transpolar Drift (TPD), a major current system transporting material from the Siberian coasts across the Arctic Ocean to Fram Strait and subsequently along the eastern coast of Greenland, at an average velocity of *ca.* 7 km per day (Krumpen *et al.* 2019). It can thus be transported over considerable distances before final deposition along Arctic coasts. However, its oceanic residence time is constrained by the buoyancy of the wood: after *ca.* 15 months of floating, most logs lose buoyancy and sink (Linderholm *et al.* 2021). Greater quantities of driftwood from western Siberia are deposited on Svalbard than on Greenland or Iceland, where material of central and eastern Siberian origin dominates. This spatial variability in driftwood deposition is primarily controlled by sea ice drift pathways and associated surface current dynamics (Linderholm *et al.* 2021).

Svalbard is well known for the large quantities of driftwood deposited along its shores. Driftwood samples collected in this region have been repeatedly utilized in a range of research projects (Hellmann *et al.* 2015, 2017; Hole *et al.* 2021; Linderholm *et al.* 2021). These studies concerned the origin, genus/species composition, and age of driftwood on Svalbard. Driftwood was also used to infer past sea-ice conditions. It has been established that *ca.* 70% of this material on Svalbard originates from the Yenisei River, with the dominant taxa being *Pinus sylvestris*, *Larix* spp., and *Picea* spp. The oldest specimens date back to the 13th century (Hellmann *et al.* 2017).

Dendrochronological analyses and tree-ring width (TRW) records from driftwood have been successfully applied as proxies for reconstructing Arctic Ocean surface circulation and sea-ice dynamics at decadal resolution over the past 500 years (Hole *et al.* 2021). Furthermore, a recent hypothesis (Węśławski *et al.* 2024) suggests that the abundance of driftwood along the coast may be correlated with the amount of plastic debris deposited on Svalbard's shores.

Despite the frequent use of Svalbard driftwood in scientific studies, its spatial distribution and the mechanisms governing it remain poorly understood. The objective of this project is to address this knowledge gap. Using model data describing sea-ice drift and surface-current dynamics, a Driftwood Transport Model (DWTM) was developed, building upon existing frameworks (Dalaiden *et al.* 2018), to simulate the transport of driftwood from the Pechora, Ob, and Yenisei rivers to the coasts of Svalbard. A detailed map of driftwood distribution across

Svalbard was produced and compared with the model output. In addition, a quantitative estimate of the total volume of driftwood deposited along Svalbard's coasts was attempted.

## Materials and methods

### Driftwood Transport Model

To track the trajectories of tree trunks entering the Arctic Ocean from the river mouths of the Pechora, Ob, and Yenisei, we applied a Lagrangian drift model for sea ice and surface waters, the Driftwood Transport Model (DWTM), which was adapted from the Drift Trajectory Model (DTM) (Dalaiden *et al.* 2018). The governing equation of the model is given as:

$$v_i(t) = \frac{dx_i(t)}{dt} \quad (1)$$

where  $x$  and  $v$  are the position and velocity of each simulated wood,  $t$  is the time.

Equation (1) is discretized using the forward Euler method, which updates particle position iteratively according to the velocity field derived from sea-ice drift and surface current data. This approach provides a computationally efficient means of approximating Lagrangian trajectories while preserving the temporal resolution required to capture driftwood transport pathways:

$$x_i(t + 1) = x_i + v_i(t) \times \Delta t \quad (2)$$

where  $\Delta t$  is one day,  $v_i(t)$  is the mean daily velocity of sea ice, or of surface water in the absence of ice.

Using Eq. (2), I simulated the drift trajectories of 2 775 tree trunks, randomly released in the estuarine regions of the three rivers at five-day intervals between May and September for the period of 1991–2016. As long as sea-ice concentration exceeded a threshold value, driftwood was assumed to drift passively with the ice, such that DW velocity equaled sea-ice velocity. When ice concentration fell below this threshold, DW velocity was set equal to the ocean surface current velocity, but only for the time span constrained by the floating capacity of the wood, after which the logs were assumed to sink (Eggertsson 1993). In the model, this buoyancy period was set to 17 months.

The DWTM was driven by sea-ice velocity and ocean current fields obtained from the Arctic Ocean Physics Reanalysis product (ARCTIC\_MULTIYEAR\_PHY\_002\_003 2023) available through the Copernicus Marine Data Store. The simulated drift trajectories were subjected to basic statistical analyses to estimate drift duration and the proportion of driftwood

reaching the coastal regions of Svalbard. In addition, kernel density estimation was applied to identify areas with the highest density of drift trajectories.

### **Mapping Driftwood Logs from Satellite Images**

Driftwood (DW) logs deposited along the coasts of Svalbard (Fig. 1) are several meters in length, allowing them to be identified in high-resolution satellite imagery. Such images can be obtained from Bing Maps Satellite Imagery and ESRI Satellite (ArcGIS/World Imagery) via various APIs. For this project, images were acquired through the QGIS interface (2009), which facilitates retrieval of the most recent and highest-quality images available for a given location. Analysis of image acquisition dates indicated that the majority of images were no older than 2–3 years. DW logs are readily identifiable due to their elongated shape, light coloration (contrasting with the background), and the shadows they cast under low solar angles.

Two separate mapping tasks were undertaken using satellite imagery. In the first task, each individual DW log was represented as a line feature in a vector model. Along a 475 km stretch of the western coast of Spitsbergen (*ca.* 6% of the Svalbard coastline), logs were digitized along five segments, resulting in a total of 20 250 individual DW logs. For each linear feature representing an individual DW log, the following attributes were recorded: elevation (from digital elevation model, DEM), distance to the shoreline, and object length (*i.e.*, DW length). Statistical and spatial analyses were subsequently performed, incorporating coastline data and DEM. The DEM for Svalbard used in this study was derived from ArcticDEM (Porter *et al.* 2018), which is based on high-resolution imagery acquired by the DigitalGlobe optical satellite.

In the second task, driftwood aggregations were digitized as polygons and classified into three density categories along the entire Svalbard coastline. A total of 11 362 polygons representing DW aggregations were created. Combining the results of these two tasks enabled calculation of the mean number of DW logs per polygon within each density class and facilitated a rough quantitative estimation of the total number of DW logs along Svalbard's coasts.

## **Results**

The results of the DWTM simulations are presented in Fig. 2. Trajectories, represented as sequences of driftwood (DW) locations generated by the model until either sinking or arrival at the coastline, are shown in Fig. 2A. Three colors indicate the river of origin for each trajectory: Pechora, Ob, and Yenisei. The direct and fastest transit along the full route, spanning 700–9 000 km from the river mouth to the map boundary off Greenland's coast, takes 26–32 months. On

average, trajectories require 40–50 months, with no significant difference based on the starting location.

Figure 2B illustrates the mean drift direction of DW logs and the density of drift trajectories, calculated using kernel density estimation, which produces a continuous map of trajectory density in km/km<sup>2</sup>. Analysis of drift probability in sea ice, depending on location, indicates values of 30–70% in the Svalbard region, while in the Barents Sea this probability falls below 30%. Sinking of DW predominantly occurs in the Barents Sea region, with *ca.* 9% of logs released from the three rivers sinking before reaching the coast. In contrast, 24% of all DW reaches the coastal zone of Svalbard.

Trajectory analysis also reveals the presence of several mesoscale eddy-like structures with diameters on the order of 500 km, located to the north and northeast of Svalbard. DW tends to circulate within these structures for roughly one year.

The mapping zones for driftwood (DW) along a 475 km stretch of the western coast of Spitsbergen are shown in Fig. 3. The distribution of DW is not uniform and exhibits distinct clusters, representing areas of high DW density. The location of these clusters within the mapped region is presented in Fig. 3A. The orange line (475 km) indicates the area where DW was digitized from satellite images. The digitized driftwood logs indicate an average density of 43 DW per kilometer of coastline. Red areas indicate clusters with the highest DW density, spanning 187 km of coastline with an average of 84 DW km<sup>-1</sup>. These areas contain 77% of all digitized DW. A representative section of a cluster, illustrating the spatial arrangement of linear DW objects (1920 DW on the map), is shown in Fig. 3B. Statistics for the attributes recorded for linear objects are presented in Fig. 4A–C.

The median elevation of DW logs (Fig. 4A) was 5.6 m, with 90% located between 2.9 and 8.1 m a.s.l. Distances from the shoreline ranged from 19 to 232 m (median 65 m), and log lengths had a median of 3.4 m, with 90% falling between 1.7 and 6.1 m. The results of digitizing driftwood (DW) aggregations as polygons, classified into three density categories (sparse, medium-density, and dense DW), along the entire Svalbard coastline are shown in Fig. 5.

Driftwood (DW) was assumed to form patches of varying density, defined by the number of DW logs per hectare. Overlaying the digitized individual DW lines onto the digitized aggregation polygons of known area and three density classes allowed calculation of the mean density for each class. The sparse driftwood class had a mean density of  $30 \pm 18$  DW ha<sup>-1</sup>, the

medium-density class  $70 \pm 60$  DW ha<sup>-1</sup>, and the dense driftwood class showed the highest density at  $130 \pm 104$  DW ha<sup>-1</sup>.

Multiplying the density by the area for all patches and summing the results yielded *ca.* 60 000 digitized DW logs, assuming the digitization accurately reflects true values. It should be noted, however, that digitization may underestimate counts in the densest areas. Nevertheless, this approach allows representation of the relative spatial distribution of DW across the individual islands of Svalbard and along the Spitsbergen coastline. The results are summarized in Table 1 below.

## Discussion

In this study, two complementary approaches were used to analyze the distribution of driftwood (DW) on Svalbard. The first approach, similar to previous studies (Dalaiden *et al.* 2018; Linderholm *et al.* 2021), employed a model that calculates sea-ice and surface water velocities, which were then used to generate DW trajectories during drift in ice and water. Simulating DW trajectories from the mouths of Siberian rivers to either the boundary of the study area or until sinking allows identification of locations where trajectories reach the coastal zone. Due to model resolution limitations, the actual deposition process at the shoreline cannot be directly simulated. Nevertheless, the density of trajectories provides a proxy for potential deposition. In practice, reaching the coastal zone was assumed to correspond to a 0.5 probability of deposition. Kernel density estimation of trajectory density was used to indicate the spatial distribution of DW deposition along the coast.

Analysis of Fig. 2 shows that the Svalbard coastline is surrounded by DW trajectories from all directions, with the highest densities observed along the northern shores of the archipelago. Model results indicate that 24% of DW transported by the Pechora, Ob, and Yenisei rivers reach the Svalbard coast. The model was run for the period 1991–2016, which partially covers a period of declining sea-ice extent. At the same time, the DW currently found along Svalbard's coasts originates from several centuries, during which sea-ice conditions likely varied. The model result of 9% of DW sinking in the Barents Sea may represent a phenomenon that was less common during periods of higher ice cover.

The second approach to analyzing DW distribution was based on digitizing their presence in high-resolution satellite imagery. An example of such an image is shown in Fig. 6. Driftwood occurrences may be either scattered or form distinct clusters. Certain coastal types

prevent DW deposition. Glaciers reaching the sea account for over 10% of the coastline, and some areas are rocky or cliffed, which excludes substantial portions of the coast from deposition. Fjord coasts are not directly exposed to incoming DW; logs must first enter the fjord, and the width of the fjord entrance represents only a small fraction of the total fjord coastline. Consequently, lower DW densities were observed within all fjords.

The satellite-based analysis involved digitizing individual DWs either as line segments representing single logs or as polygons covering areas with approximately homogeneous DW density. The first method encompassed five selected stretches along a 475 km section of the western coast of Spitsbergen (Fig. 3A). Results from this line-based digitization revealed a clear clustering of DWs (Fig. 3B).

However, digitization of dense DW clusters as individual logs is limited by their high concentration, making it impossible to identify every log. This limitation is illustrated in Fig. 6, where a dense aggregation is indicated by a red arrow. Nonetheless, statistically significant numbers of DWs were successfully digitized as line segments, allowing analysis of log lengths (Fig. 4C), as well as their elevation relative to the DEM and distance from the shoreline. DWs measured between 3 and 8 m, corresponding to the typical size range of softwood sawlogs (pine, spruce, larch) in practice (3–6 m, maximum 12 m; OpenAI 2025). Values below 3 m observed in the histogram (Fig. 4C) likely represent broken logs or anthropogenic wood debris.

The elevation at which DWs are found is influenced by deposition mechanisms, including typical tides (maximum 1 m in Hornsund) and storm surges (extremes up to 4 m) (Kristensen *et al.* 2023; Swirad *et al.* 2023). Storm wave action in the coastal zone and potential errors in the DEM must also be considered. In addition, because Svalbard was partially glaciated during the Last Glacial Maximum, the region is subject to isostatic adjustment, with a typical vertical uplift rate of 2–7 cm per decade (Bungenstock *et al.* 2021; Kierulf *et al.* 2022). Therefore, the elevation range observed in the histogram (Fig. 4A; 90% of data between 3–8 m) appears reasonable.

Distances from the shoreline (Fig. 4B) are controlled by coastal morphology. DW logs may be deposited behind beach ridges in long linear formations, as shown in Fig. 3B. Under extreme sea-level conditions, logs can also be transported upriver or into adjacent lagoons, where they are deposited along river or lagoon margins. In lagoons, wind-driven drift may further concentrate DWs along former shorelines once water levels recede (Fig. 6, red arrow). Such accumulations are commonly observed along Svalbard's coasts.

The second satellite-based mapping method assigned DW aggregations to three relative density classes (sparse, medium-density, and dense driftwood), enabling analysis of DW distribution along the entire Svalbard coastline. By overlaying the polygons on digitized line features, the mean density for each class could be determined, and, given the known polygon areas, the number of DWs per polygon could be estimated. However, large standard deviations within each class and underestimation in the densest class introduce substantial uncertainty to these quantitative estimates.

Figure 5 shows the spatial distribution of DWs across Svalbard. The distribution is clearly clustered, with pronounced gaps corresponding to the fronts of large glaciers (e.g., on Nordaustlandet and Edgeøya). A distinct zone of high dense-driftwood occurrence is observed along the northern coasts of Spitsbergen and Nordaustlandet, coinciding with the region of highest trajectory density identified in Fig. 2B. This area contains 32% of all DWs on Svalbard. A second continuous area of very high DW abundance is Prins Karls Forland, which contains 24% of Svalbard's DWs, representing a major component of the entire western coast of Spitsbergen (48% of DWs). Notably, most fjords show low or negligible DW presence.

The total number of DWs across Svalbard is estimated to range from *ca.* 100 000 to 300 000. This estimate accounts for underestimation in the densest class, variability indicated by standard deviations, and uncertainties in areas obscured by snow, ice, or clouds. Consequently, this range carries potentially large errors and is provided primarily to illustrate the scale of the phenomenon.

Since Stadié *et al.* (2025) used similar methods for analyzing DW along the Arctic coasts of Alaska and Northwest Canada, the results of both studies can be compared. They found that along the *ca.* 8 800 km of coastline they examined (at a defined level of detail), large-scale distribution patterns of DW form clusters near major river deltas. They also concluded (Stadié *et al.* 2025) that long-range transport of DW by sea ice and ocean currents, with some logs reaching distant locations such as Svalbard, is an exception rather than the norm, which is deposition close to the riverine source.

The results presented for Svalbard contradict the claim that long-range transport plays only a minor role. Model simulations indicate that 24% of the DW transported by the three major Siberian rivers reaches the coasts of Svalbard. The mean surface area of deposited driftwood per kilometre of coastline is 2 400 m<sup>2</sup> per km for Svalbard and 2 600 m<sup>2</sup> per km for the North American coast, with deposition clustering observed in both cases. For North America, clustering

is primarily controlled by distance from river mouths, whereas on Svalbard it is driven by coastline morphology and circulation patterns. Cluster sizes are also comparable, with mean values of 880 m<sup>2</sup> on Svalbard and 1 164 m<sup>2</sup> along the North American coast.

## Conclusions

This study provides the first archipelago-wide assessment of driftwood distribution on Svalbard by integrating numerical driftwood transport modelling with systematic satellite-based mapping. The strong spatial correspondence between modeled transport pathways and observed coastal deposition patterns demonstrates that large-scale ocean and sea-ice circulation exerts a primary control on driftwood delivery to the archipelago.

Model results indicate that a substantial fraction of driftwood released from major Siberian rivers can reach Svalbard, with roughly one quarter of simulated trajectories intersecting the coastal zone. Areas of highest modeled trajectory density coincide with the northern coasts of Spitsbergen and Nordaustlandet, where satellite mapping reveals the densest driftwood accumulations. This agreement supports the interpretation that Svalbard functions as an important terminal sink for Siberian driftwood within the Arctic system.

Satellite observations further show that driftwood deposition is highly clustered and strongly constrained by coastal morphology. Accumulation is favored along exposed shorelines, beach ridges, and low-relief coastal environments, whereas steep rocky coasts, fjords, and tidewater glacier fronts largely inhibit deposition. These patterns indicate that final driftwood emplacement is governed by shoreline geometry and extreme marine processes rather than uniform coastal transport.

Estimated driftwood abundances of *ca.* 100 000 to 300 000 logs highlight the magnitude of long-distance driftwood transport to the High Arctic. In contrast to Arctic North America, where deposition is closely linked to proximity to river sources, driftwood patterns on Svalbard are primarily controlled by pan-Arctic circulation and coastal setting.

Overall, the results demonstrate that long-range driftwood transport to Svalbard is not exceptional but reflects strong connectivity within the Arctic Ocean system. This connectivity underscores the sensitivity of driftwood delivery and deposition to changes in sea-ice dynamics and ocean circulation under future climate conditions.

## Acknowledgements

The author would like to thank the reviewers for their helpful comments and insightful suggestions. The following projects supported author: *MARBEFES – MARine Biodiversity and Ecosystem Functioning Leading to Ecosystem Services*, European Union's Horizon Europe research and innovation programme under Grant Agreement no 101060937; partly supported by Miljøvernfond project nr 23/12 RIS 12284.

## References

- ARCTIC\_MULTIYEAR\_PHY\_002\_003. *E.U. Copernicus Marine Service Information (CMEMS) Marine Data Store (MDS)*, doi: 10.48670/moi-00007, accessed 1.08.2023.
- Bungenstock F., Kaufmann G. and Klemann V. 2021. Post-glacial rebound in Svalbard observed with continuous GPS and tide gauge measurements. *Journal of Geodynamics* 149: 101811, doi: 10.1016/j.jog.2021.101811.
- Dalaiden Q., Goosse H., Lecomte O. and Docquier D. 2018. A model to interpret DW transport in the Arctic. *Quaternary Science Reviews* 191: 89–100, doi: 10.1016/j.quascirev.2018.05.004.
- Eggertsson Ó. 1993. Origin of the driftwood on the coasts of Iceland: A dendrochronological study. *Jökull* 43: 24–32, doi: 10.33799/jokull1993.43.015.
- Hellmann L., Tegel W., Geyer W., Kirilyanov A., Nikolaev A., Eggertsson O., Altman J., Reinig F., Morganti S., Wacker L. and Büntgen U. 2017. Dendro-provenancing of Arctic DW. *Quaternary Science Reviews* 162: 1–11, doi: 10.1016/j.quascirev.2017.02.025.
- Hellmann L., Tegel W., Kirilyanov A.V., Eggertsson Ó., Esper J., Agafonov L., Nikolaev A.N., Knorre A.A., Myglan V.S., Churakova (Sidorova) O., Schweingruber F.H., Nievergelt D., Verstege A. and Büntgen U. 2015. Timber logging in central Siberia is the main source for recent Arctic DW. *Arctic, Antarctic, and Alpine Research* 47: 449–460, doi: 10.1657/AAAR0014-063.
- Hole G.M., Rawson T., Farnsworth W.R., Schomacker A., Ingolfsson O. and Macias-Fauria M. 2021. A DW-based record of Arctic sea ice during the last 500 years from northern Svalbard reveals sea ice dynamics in the Arctic Ocean and Arctic peripheral seas. *Journal of Geophysical Research: Oceans* 126: e2021JC017563, doi: 10.1029/2021JC017563.e.
- Kierulf H.P., Kohler J., Boy J., Geymann E.C., Memin A., Omang O.C.D., Steffen H. and Steffen R. 2022. Time-varying uplift in Svalbard – an effect of glacial changes. *Geophysical Journal International* 231: 1518–1534, doi: 10.1093/gji/ggac264.
- Kristensen N.M., Tedesco P., Rabault J., Aarnes O. J., Sætra Ø. and Breivik Ø. 2023. NORA-Surge: A storm surge hindcast for the Norwegian Sea, the North Sea and the Barents Sea. *arXiv preprint*, December 18, 2023. doi: 10.48550/arXiv.2312.11585.
- Krumpen T., Belter H.J., Boetius A., Damm E., Haas C., Hendricks S., Nicolaus M., Nothig E.M., Paul S., Peeken I., Ricker R. and Stein R. 2019. Arctic warming interrupts the Transpolar Drift and

- affects long-range transport of sea ice and ice-rafted matter. *Scientific Reports* 9: 5459, doi: 10.1038/s41598-01941456-y.
- Linderholm H.W., Gunnarson B.E., Fuentes M. and Büntgen U. 2021. The origin of DW on eastern and south-western Svalbard. *Polar Science* 29: 1–9, doi: 10.1016/j.polar.2021.100658.
- OpenAI 2025. ChatGPT (September 2 version) [Large language model]. <https://chat.openai.com/OpenAI>.
- QGIS Development Team 2009. QGIS Geographic Information System. Open Source Geospatial Foundation, <http://qgis.org>.
- Porter C., Morin P., Howat I.N., Myoung-Jon B., Peterman K.S., Schlenk M., Gardiner J., Tomko K., Willis M., Kelleher C., Cloutier M., Husby E., Foga S., Nakamura H., Platson M., Wethington M., Williamson C., Bauer G., Enos J.A., Kramer W., Becker P., Doshi A., D’Souza C., Cummins P., Laurier F. and Bojesen M. 2018. ArcticDEM, doi: 10.7910/DVN/OHHUKH, Harvard Dataverse, V1, accessed 1.08.2021.
- Stadie C. Brandt M., Nitze I., Tong X., Liu S., Kariryaa A., Li S., Reiner F., Rettelbach T. and Grosse G. 2025. Large driftwood accumulations along Arctic coastlines and rivers. *Scientific Reports* 15: 32500, doi: 10.1038/s41598-025-17426-y .
- Swirad Z.M., Moskalik M. and Herman A. 2023. Wind wave and water level dataset for Hornsund, Svalbard (2013–2021). *Earth System Science Data* 15: 2623–2633, doi: 10.5194/essd-15-2623–2023.
- Węśławski J.M., Urbański J. and Kotwicki L. 2024. *Satellite Imagery of driftwood on Svalbard as Proxy for Plastic Litter Deposition. First Assessment.* Available at SSRN: <https://ssrn.com/abstract=4735462>, doi: 10.2139/ssrn.4735462.

**Table 1.** Distribution of driftwood across Svalbard.

| Area                 | Total driftwood on Svalbard (%) |
|----------------------|---------------------------------|
| Nordautlandet        | 12                              |
| Barentsøya           | 2                               |
| Edgeøya              | 9                               |
| Prins Karls Forland  | 24                              |
| Spitsbergen          | 53                              |
| N coasts of Svalbard | 32                              |
| W coasts of Svalbard | 48                              |
| E coasts of Svalbard | 6                               |



**Fig. 1.** Driftwood (DW) depositions: **A** – medium-density DW along the coast on a beach ridge; **B** – dense DW; **C** – sparse DW on a flat coastal area; **D** – dense DW forming a belt along a dried lake, with visible plastic debris (photo: Institute of Oceanology PAN).

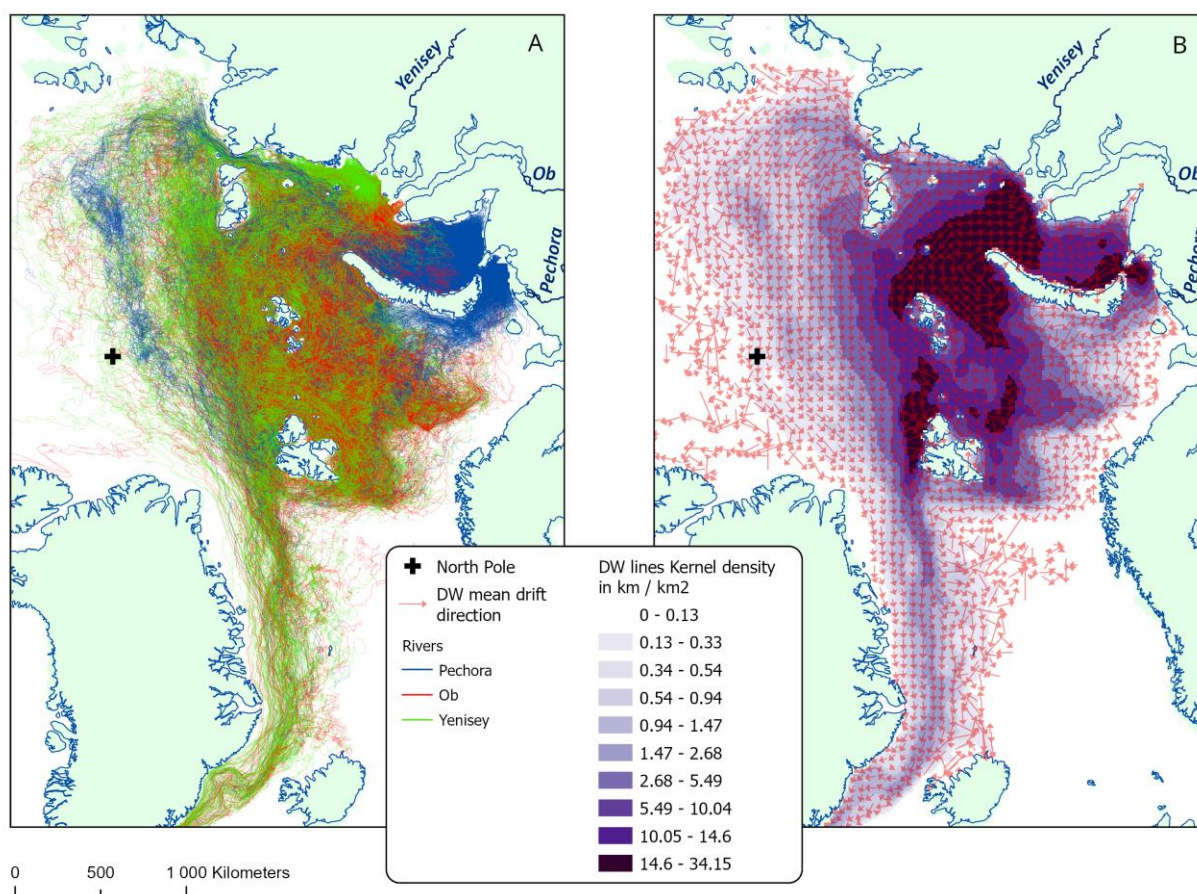


**Fig. 2.** Driftwood (DW) transport model results: **A** – trajectories of 2 775 wood logs released from the estuarine regions of three rivers: Pechora, Ob, and Yenisei and **B** – mean drift direction of wood logs in sea ice and water, and kernel density of DW trajectories (km km<sup>-2</sup>).

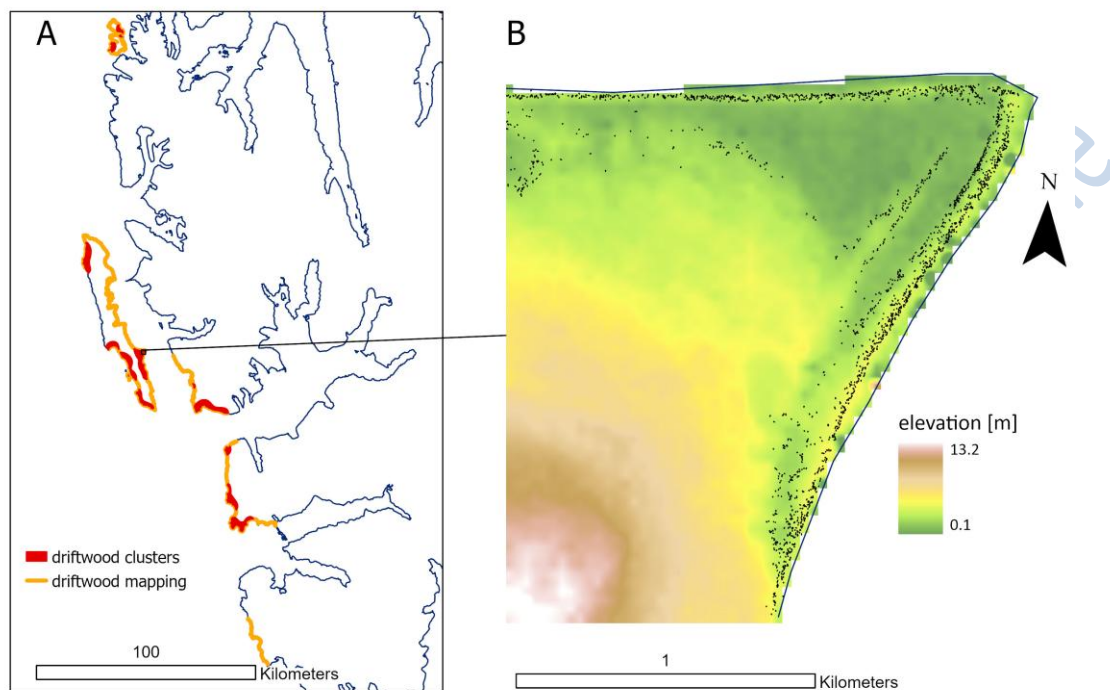


**Fig. 3.** Mapping of driftwood as line features: **A** – location of the five mapping zones along the western coast of Spitsbergen, with high-density clusters highlighted in red and **B** – example of a driftwood cluster in the Poolepynten area (Prins Karls Forland) overlaid on a raster DEM layer.

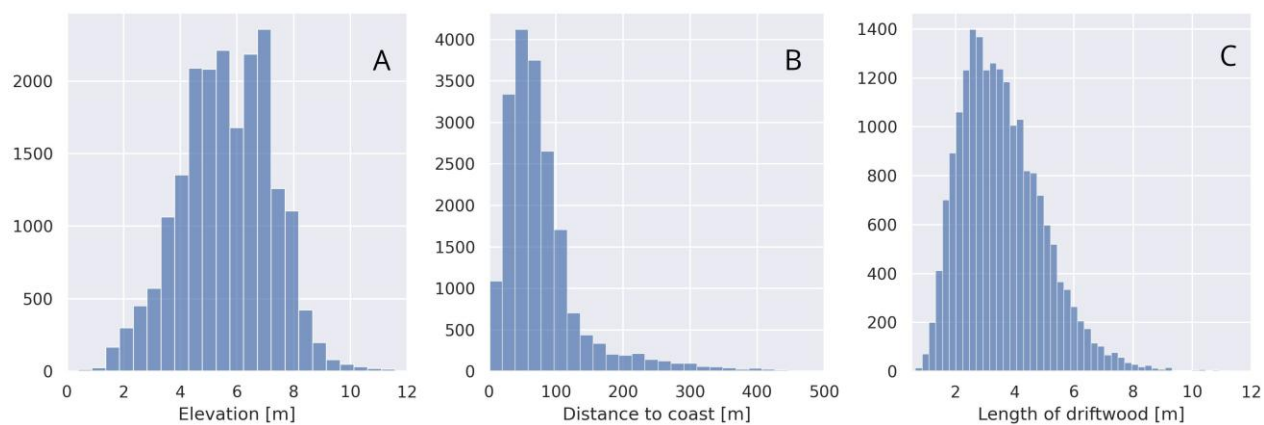


**Fig. 4.** Histograms of attributes for digitized driftwood logs: **A** – elevation, **B** – distance to the coastline, and **C** – log length.

Polish Polar Research - Accepted Article

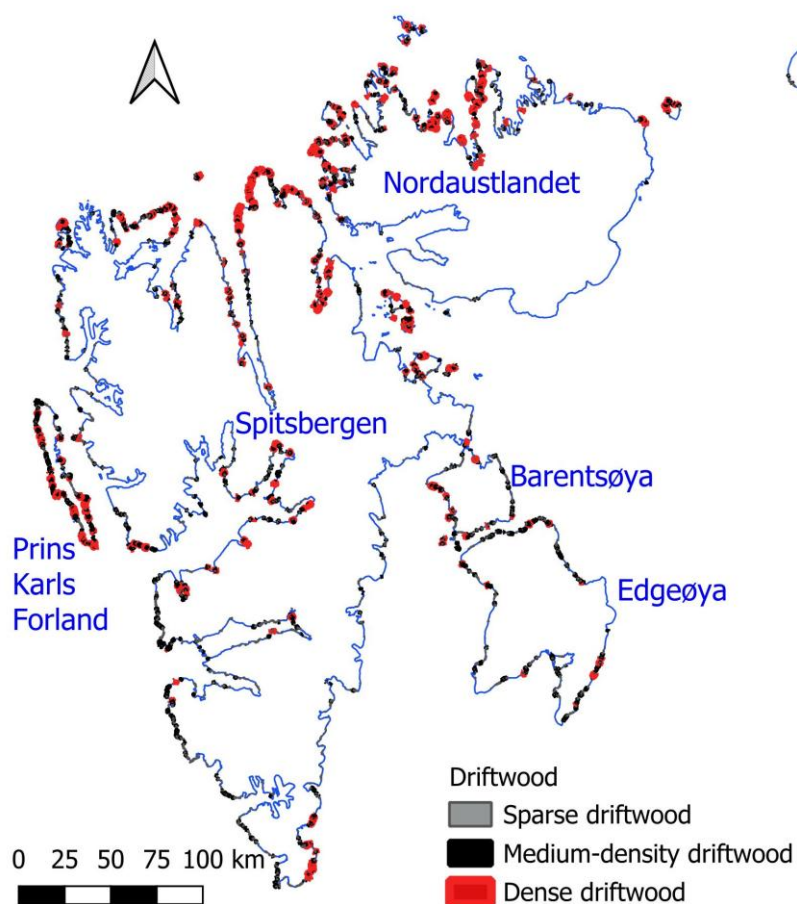


**Fig. 5.** Distribution of driftwood on Svalbard. Driftwood aggregations are shown in three density classes: sparse, medium-density, and dense.

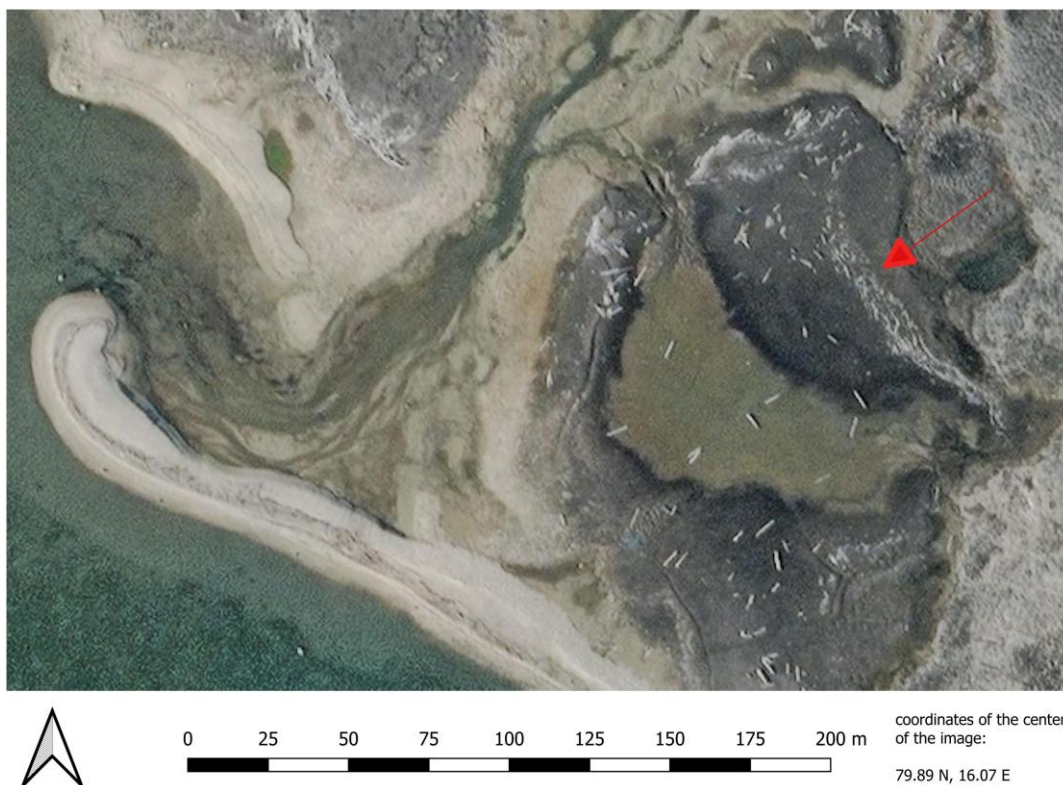


**Fig. 6.** Satellite image of the Svalbard coastline (Polheimhamna, Ny Friesland, northern Spitsbergen, centered at 79.89°N, 16.07°E). Red arrow indicates an example of driftwood accumulation along a lagoon shoreline.